Efficient Computation of Phase Equilibria in Polydisperse Polymer Solutions Using *R*-Equivalent Δ-Function Molecular Weight Distributions

Peter A. Irvine and John W. Kennedy*

Department of Chemistry, Stanford University, Stanford, California 94305, Department of Statistics, Baruch College of the City University of New York, New York, New York 10010, and University of Essex, Colchester CO4 3SQ, Essex, England. *Received March 19, 1981*

ABSTRACT: A convenient and useful way of approximating any polymer molecular weight distribution (MWD), even if it is formally unbounded in terms of the number of components, is via its *R*-equivalent analogue comprising approximately $R/2$ Δ-function components. This approximation allows us to match just *R* moments of the Δ-function distribution to those of the original MWD (though, of course, the Δ-function distribution also has infinitely many other moments that do not match in general). The usefulness of this device lies in the fact that efficient computational procedures can then be employed to evaluate physical properties expressed as series expansions in the moments of the MWD. Though such expansions formally involve infinitely many moments (and hence terms), in many cases convergence is rapid and in some cases exact after the first few terms. We illustrate these ideas with reference to computation of loci in phase equilibria diagrams for polymer solutions from theoretical free energy of mixing functions in the manner prescribed by J. W. Gibbs. In the case of spinodal and critical point loci, substantial computational labor is saved by a restatement of the Gibbs criteria in the language of linear algebra. Furthermore, for a class of commonly used free energy of mixing functions it has been proven elsewhere that these two loci depend explicitly on a well-defined finite set of moments so that exact truncation of the moment expansions apply. For cloud point curves (CPC) and associated features such as phase volume ratios and Breitenbach–Wolf plots, no strict truncation seems possible so accuracy must be improved by increasing the number *R* of exactly specified moments of the MWD. Numerical calculations indicate that the rate of convergence in these cases is strongly affected by polydispersity. Whereas the CPC for a true Flory MWD and that for its *R*-equivalent approximation differ little beyond $R = 8$, much larger values for *R* are required when modeling the very broad log-normal distribution.

1. Introduction

In 1968 Koningsveld and Staverman published a series of papers[1] describing the detailed computation of thermodynamic phase equilibria loci for polydisperse polymer solutions from theoretical (free energy of mixing) ΔG functions according to the criteria propounded by Gibbs.[2] These loci are discussed in the present paper and together they offer the possibility for indirect experimental study of the first three derivatives of ΔG with respect to concentration. Spinodal loci, involving the second derivative, have been particularly well studied due mainly to the relative simplicity of computation and the ease of measurement.[3,4] As is further evident from this work, spinodal loci exhibit a level of sensitivity to the form theoretical ΔG functions which is just about appropriate to the meaningful testing of these functions in their present state of development. This ranking of phase equilibria measurements by sensitivity to the form of ΔG and the conclusions for testing theoretical ΔG functions has been discussed elsewhere.[5]

The main purpose of the present paper is to detail computational developments announced previously.[6] Specifically, these center on dealing efficiently with polymer systems in which the polymer MWD implies essentially infinitely many species and hence the system has infinitely many distinct thermodynamic components. Our computational gains are achieved by sacrificing information on all but *R* selected moments of the MWD, a procedure which in certian cases has been proven[7] to involve no approximation. By adopting this policy we replace the infinite system by a finite *R-equivalent system* comprising $[R/2]$ Δ-function polymer components. ($[x]$ is the smallest integer not less than x.) Phase equilibria loci can then be computed directly and with facility to varying degrees of approximation depending on the number *R* of constrained (that is, exactly represented) moments.

Part 2 describes the numerical construction of *R*-equivalent Δ-function distributions and the algorithms for computation of phase equilibria based thereon. The latter include details of a simplified matrix computation of spinodal and critical loci. The numerical calculations presented in part 3 are designed to illustrate how the *R*-equivalent approximation manifests itself in computer phase equilibria and the accompanying influence of polydispersity on phase loci.[8] More specific details concerning the algorithms used and the calculations performed are offered in the appendices.

2.1. *R*-Equivalent Δ-Function Distributions

The *k*th moment (about the origin) of a molecular weight distribution (MWD) is defined thus for a mixture of *n* polymer components:

$$M_k = \sum_{i=1}^{n} w_i m_i^k \tag{1}$$

where w_i is the weight fraction and m_i the molecular weight of polymer species *i*. The distribution is normalized if $M_0 = 1$ and, of course, we may always scale the moments so that this normalization condition is met. We define two distributions to be *R*-equivalent if they possess identical sets of *R* specified moments $\{M_{\mathbf{R}}\}$ (including M_0), but they may differ in others.

$$\{M_{\mathbf{R}}\} \equiv \{M_{r_\alpha};\ \alpha = 1, 2, \ldots, R;\ r_1 < r_2 < \ldots < r_R | r_\alpha = 0 \text{ for some } \alpha\} \tag{2}$$

However, for convenience, we shall restrict ourselves to sets of *consecutive moments of integral order*, viz.

$$\{M_{\mathbf{R}}^{(s)}\} \equiv \{M_s, M_{s+1}, \ldots, M_{R+s-1}\} \tag{3}$$

with *s* typically equal to 0 or −1.

A convenient choice for a theoretical distribution which is *R*-equivalent to some specified arbitrary distribution is

* To whom correspondence should be addressed at the Research Institute, Advanced Medical Products, 10 Conway Close, Clacton-on-Sea, Essex, England.

0024-9297/82/2215-0473$01.25/0

Table I
Computed R-Equivalent Δ-Function Distributions Based on Exact Matching of Moments $\{M_R^{(0)}\}$ to Those of Flory (F) and Log-Normal (LN) Distributions Normalized with $M_1 = 2.0 \times 10^5$ and $p_1 = 1.5$ (See Text)

		R-equivalent Δ-function distribution $\{w_{R*}, m_{R*}\}$							
R	MWD	w_1	$m_1 \times 10^{-5}$	w_2	$m_2 \times 10^{-5}$	w_3	$m_3 \times 10^{-5}$	w_4	$m_4 \times 10^{-5}$
2	F	1.0	2.0						
	LN	1.0	2.0						
4	F	0.21133	4.732	0.78867	1.268				
	LN	0.11111	6.000	0.88889	1.500				
6	F	0.02010	7.759	0.39122	3.305	0.58868	0.936		
	LN	1.58×10^{-3}	15.57	0.21164	4.500	0.78678	1.300		
8	F	1.32×10^{-3}	10.95	0.07418	5.731	0.47764	2.572	0.44687	0.743
	LN	4.0×10^{-6}	38.04	5.82×10^{-3}	11.71	0.27521	3.890	0.71897	1.198

one synthesized from a mixture of Δ functions. In this case the R-equivalent distribution comprises $[R/2]$ components, each of whose weight fraction and molecular weight are *uniquely* specified (see Appendix 2) as the solution (see Appendix 1) of the R simultaneous nonlinear equations

$$\sum_{i=1}^{R/2} w_i m_i^k = M_k; \qquad k = s, s+1, ..., R+s-1 \quad (4)$$

which define the moments in the set $\{M_R^{(s)}\}$. The same system of equations (4) arise also in the Gaussian quadrature method of numerical integration[9] and can be solved by an elegant polynomial algorithm (Appendix 1). The set of $R^* \equiv [R/2]$ Δ-functions that represent the solution to eq 4 we denote by $\{w_{R^*}, m_{R^*}\}^{(s)}$.

Numerical examples of R-equivalent Δ-function distributions based on sets of consecutive moments of integral order (eq 3) are offered in part 3 (cf. Table I). We are unaware of any numerical method that will deal with solving the general R-equivalent case that matches an arbitrarily selected set of moments $\{M_R\}$ (see eq 2).

2.2. Computation of Quasi-Binary Phase Diagrams

Theoretical models for the thermodynamic behavior of polydisperse polymer solutions are usefully summarized in terms of the free energy of mixing (or ΔG) functions to which they lead. Most of these functions explicitly include the entropy of mixing terms proposed independently by Huggins[10] and by Flory[11] and any G function can be formally written so as to display those terms. It is convenient, therefore, to express ΔG functions as a generalized form of the Flory–Huggins expression.[4,6,12,13] For a quasi-binary[14] system, this may be written

$$\Delta G^+ \equiv \Delta G/R_g TV = \phi_0 \ln \phi_0 + \sum_i \phi_i c m_i^{-1} \ln \phi_0 + \Gamma \quad (5)$$

where R_g is the gas constant, T the absolute temperature, V the volume of the solution, ϕ_0 the volume fraction of solvent, and ϕ_i that of the ith polymer component. The ratio c of the molar volume of a polymer repeat unit to that of the solvent is, in effect, a constant for the polymer/solvent system that converts molecular weights to statistical chain lengths. The development of more refined models is charted in the evolving form of the interaction funtion g[6,8] present in the exess (interaction) term Γ:

$$\Gamma = \phi_0 \phi g(T, \{M_R^{(s)}\}) \quad (6)$$

For the important class of ΔG functions (eq 5 and 6) in which the set $\{M_R^{(s)}\}$ of eq 6 is *of finite order* there are highly efficient computational procedures for locating the various loci of the phase diagram. This highlights the reason for our use of the generalized Flory–Huggins form for ΔG (eq 5) since the entropy of mixing terms therein cannot themselves be expressed as a function of any finite set of moments of the molecular weight distribution. The computational procedures are now described.

2.2.1. Spinodal and Critical Loci. Following Gibbs (ref 2, but see also ref 4), points on the spinodal locus $\{\phi_{sp}, T_{sp}\}$, or limit of metastability for homogeneous solutions, are characterized by

$$J_{sp} \equiv |(\partial^2 \Delta G^+/\partial\phi_i \partial\phi_j)_{T,P}| = 0; \qquad i, j = 1, 2, ... \quad (7)$$

Similarly, in a critical point (ϕ_{cr}, T_{cr}), which is also a spinodal point, the determinant J_{cr} is equal to zero in addition, where J_{cr} is obtained by replacing the elements of *any* line (row or column) of J_{sp} by those of the vector $\{(\partial J_{sp}/\partial\phi_i)_{T,P}; i = 1, 2, ...\}$. In general, polymer molecular weight distributions imply the existence of infinitely many polymer components, so the two determinants J_{sp} and J_{cr} are formally of infinite order.

For ΔG functions (eq 5) whose interaction term (eq 6) depends on a *finite* set of moments $\{M_R^{(s)}\}$ (defined in eq 3), two truncation theorems[7] lead to the following results:

$$T_{sp} = T_{sp}(M_s, M_{s+1}, ..., M_{2(R+s)-1}) \quad (8)$$

$$T_{cr} = T_{cr}(M_s, M_{s+1}, ..., M_{3(R+s)-1}) \quad (9)$$

In words, when the ΔG function depends only on integral order moments M_s through $M_{(R+s)-1}$, T_{sp} depends on, and only on, all integral order moments M_s through $M_{2(R+s)-1}$. Similarly, T_{cr} depends on moments up to $M_{3(R+s)-1}$. In the absence of any such truncation, exact computation of these phase loci would require complete knowledge of the MWD (i.e., knowledge of all moments), so it would not be possible to avoid the use of infinite-order determinants J_{sp} and J_{cr}.

It having been demonstrated that T_{sp} and T_{cr} depend on only a finite (usually small) set of moments, we are free to compute these temperatures *using any distribution which shares the same set of prescribed moments.* Thus, for the cases above (eq 8 and 9), we need only to replace an infinite MWD by R-equivalent Δ-function distributions with $[(2R+s)/2]$ and $[(3R+s)/2]$ components, respectively. An equivalent reduction in the orders of the two determinants is now immediate. Thus J_{sp} is replaced by

$$J_1 = J_1\{w_{R^*}, m_{R^*}\}; \qquad R^* = [(2R+s)/2] \quad (10)$$

and J_{cr} is replaced by

$$J_2 = J_2\{w_{R^*}, m_{R^*}\}; \qquad R^* = [(3R+s)/2] \quad (11)$$

The R-equivalent spinodal determinant J_1 of order $[(2R+s)/2]$ is just the product of eigenvalues of the associated matrix $\tilde{J}_1$. For fixed $\phi = \phi_{sp}$ the spinodal temperature, T_{sp}, is now simply the temerature at which the smallest eigenvalue λ_0 of $\tilde{J}_1$ takes the value zero. Efficient algorithms are available for evaluating the smallest eigenvalue of a matrix (see Appendix 3) and the search for a zero value is easily performed by a bisection method based on testing the sign of λ_0 as a function of temperature. The critical point could be located by analogously searching for a zero value of the smallest eigenvalue of the unsymmetric matrix

$\tilde{J}_2$. A more efficient method, however, exploits the directional properties of the eigenvector $\tilde{\xi}_0$ associated with the smallest eigenvalue λ_0 *of the corresponding spinodal matrix, now of order* $q \geq [(3R + s)/2]$.

In the q-dimensional composition space $(\phi_1, \phi_2, ..., \phi_q)$ associated with the critical point (and spinodal) equivalent system of Δ functions, the ith row of J_1 is the gradient vector $\tilde{\nabla}\mu_i^+$ of the scalar field $(\partial\Delta G^+/\partial\phi_i)$, itself implicitly related to the chemical potentials μ_i of the q polymer species. The spinodal determinant J_1 is a continuous scalar function in this composition space, and at a spinodal point, where $J_1 = 0$, the q gradient vectors no longer form a basis which spans this q-dimensional space but are "compressed" into a $(q-1)$-dimensional subspace. That is, only $q - 1$ of the q gradient vectors are then linearly independent. As suggested by Gibbs,[2] substitution of the gradient vector $\tilde{\nabla}J_1 \equiv \{(\partial J_1/\partial\phi_i); i = 1, 2, ..., q\}$ for any line in J_1 yields a new determinant J_2 which vanishes at the critical point. Consequently (since the critical point is also a spinodal point), at T_{cr}, $\tilde{\nabla}J_1$ is linearly related to the q linearly related gradient vectors $\tilde{\nabla}\mu_i^+$ and *so lies in the same* $(q-1)$*-dimensional subspace they span.* At other spinodal points, $\tilde{\nabla}J_1$ does not lie in this subspace but has a finite component orthogonal to it. Fortunately, this is just the direction of the eigenvector ξ_0 associated with the vanishing eigenvalue (λ_0) of $\tilde{J}_1$.

It is straightforward to test numerically whether a spinodal point is also critical by evaluating the magnitude of the component of $\tilde{\nabla}J_1$ along the eigenvector $\tilde{\xi}_0$. An extrapolation procedure then determines the critical concentration ϕ_{cr} and using this the spinodal condition yields the temperature T_{cr} (see Appendix 3).

2.2.2. Cloud Point Curves. The cloud point curve (CPC) is the locus of points $\{\phi_{cl}, T_{cl}\}$ marking incipient phase separation of an initially homogeneous solution. Thermodynamics requires that the chemical potential for each species be the same in all coexisting phases. Thus, for two (liquid–liquid) phase separation

$$\Delta\mu_0' = \Delta\mu_0'' \qquad \text{(solvent)}$$
$$\Delta\mu_i' = \Delta\mu_i''; \qquad i = 1, 2, ... \tag{12}$$

where $\Delta\mu_i$ is the chemical potential, relative to a standard reference state, divided by R_gT. In eq 12, the single and double primes denote the two coexisting phases commonly termed "principal" and "conjugate", respectively. The chemical potential of species i is, of course, the first partial derivative of the free energy ΔG (eq 5) with respect to the number of moles n_i, related to the volume fraction ϕ_i by

$$\phi_i = \frac{n_i(m_i/c)}{n_0 + \sum_k n_k(m_k/c)} \tag{13}$$

Let ϕ_i be the volume fraction of polymer species i in the initial solution, that is, prior to any phase separation. Let ϕ $(=\sum_i\phi_i)$ be similarly the total volume fraction of polymer. Obviously

$$\phi_i = \phi w_i \tag{14}$$

where w_i is the weight fraction of polymer species i, so the volume fractions in the initial solution are fully determined by the polymer MWD. Since, *at* the cloud point temperature a negligible amount of conjugate phase appears, trivial application of the mass-balance conditions leads to

$$\phi_i' = \phi_i; \qquad i = 1, 2, ...$$

and

$$w_i' = w_i; \qquad i = 1, 2, ... \tag{15}$$

so the volume fractions ϕ_i' for polymer species in the principal phase are likewise fully specified by the initial polymer MWD. Consequently, the cloud point computation now amounts to solving the set of chemical potential equations (12) with respect to temperature T and $\{\phi_i''; i = 1, 2, ...\}$.

Unlike spinodal and critical loci, the system of equations (12) does not suggest to us a truncation theorem for the moment expansion of the CPC for any ΔG function, except *in* a critical point through which the CPC passes. In the absence of a truncation result it follows that exact computation of the CPC requires complete knowledge of the MWD and poses an infinite system of equations (12). Realization that a moment expansion of the CPC truncates exactly in the critical point and must show similar convergence characteristics near a critical point encourages us to compute approximations to the CPC based on truncating its moment expansion after R terms, thereby confining the problem to a finite subset $\{M_{\mathbf{R}}^{(s)}\}$ of the complete distribution. In this way we can use the equivalent Δ-function distribution $\{w_{\mathbf{R}^*}, m_{\mathbf{R}^*}\}^{(s)}$ and then solve, without further approximation, the redued system of $([R/2] + 1)$ chemical potential equations (cf. eq 10 and 11). This procedure, based on truncation after R terms, turns out to be useful in that, as we shall show (part 3), the solution to the system of equations converges smoothly with increasing R, though less rapidly and hence requiring larger R as we move along a CPC away from a critical point. The truncated system of CPC equations is solved numerically by using a readily available root-finding subroutine for nonlinear equations (Appendix 4).

2.2.3. Phase Volume Ratios and Breitenbach–Wolf Plots. Two important, experimentally accessible features associated with phase separation (below the CPC) are (1) the ratio Q of the volumes (V' and V'') of the coexisting phases and (2) the MWD in each phase. The Breitenbach–Wolf (B–W) equation[15]

$$\ln (w_i'/w_i'') = \ln Q - \sigma_i m_i \tag{16}$$

expresses quantitatively, by means of the coefficients σ_i, the partitioning of each species i between the two phases. The phase volume ratio Q is defined by the equivalent relations:

$$Q = V'/V'' = ((\hat{w}_0 - \hat{w}_0'') + k_{sp}\sum_i(\hat{w}_i - \hat{w}_i''))/$$
$$(\hat{w}_0'' + k_{sp}\sum_i\hat{w}_i'') = (\phi'' - \phi)/(\phi - \phi') \tag{17}$$

The only parameter that must be specified for a particular polymer/solvent system is k_{sp}, the ratio of specific volume of polymer to that of solvent. The $\hat{w}$'s are to be regarded as weights rather than weight fractions. For our calculations we arbitrarily set $\hat{w}$, the total weight of all polymer species, equal to unity and determine $\hat{w}_0$ from the total polymer concentration ϕ using

$$\hat{w}_0 = k_{sp}((1 - \phi)/\phi)\hat{w} = k_{sp}((1 - \phi)/\phi) \tag{18}$$

Computation of the B–W plot is similar to that for the CPC (Appendix 4). For some choice of R and $\{M_{\mathbf{R}}^{(s)}\}$, with fixed ϕ and T $(<T_{cl})$, the equivalent Δ-function distribution is used, and the truncated system of $([R/2] + 1)$ chemical potential equations (12) is solved with respect to the weights $\hat{w}_i''$ $(i = 0, 1, ..., [R/2])$ in the conjugate phase subject to the mass-balance constraint

$$\hat{w}_i' + \hat{w}_i'' = \hat{w}; \qquad i = 0, 1, ..., [R/2] \tag{19}$$

The phase volume ratio Q can be obtained as $\ln Q$ from the intercept in the B–W plot (eq 16). This plot is linear if $\sigma_i = \sigma$ for all i, that is, if the distribution coefficient is

independent of molecular weight. More realistically, however, this coefficient does depend on molecular weight and consequently eq 16 is nonlinear, so it is easier to compute Q directly from its defining equation (17) (see Appendix 4).

3. Numerical Calculations

The numerical calculations in this section are intended to illustrate the computational procedures discussed in part 2. For this purpose we will use two ΔG functions written in generalized Flory–Huggins form (eq 5 and 6), both of them having an interaction term that depends on a *finite* set of moments $\{M_R^{(s)}\}$ as expressed in eq 3. Specifically, we perform the computations for linear polystyrene/cyclohexane systems, the polymer having either a Flory (F) or log-normal (LN) molecular weight distribution, to which we find R-equivalent Δ-function distributions.

Let $\bar{M}_k$ denote the kth molecular weight average ($= M_k/M_{k-1}$). Define, as is common, p_k to be the kth *polydispersity index* or ratio of the $(k+1)$th to kth molecular weight averages:

$$p_k = \bar{M}_{k+1}/\bar{M}_k = (M_{k+1}M_{k-1})/(M_k^2); \qquad k = 1, 2, \ldots$$
$$p_{-1} \equiv \bar{M}_1/\bar{M}_{-1} \tag{20}$$

then the important properties of the two MWD functions can be summarized, for our purposes, as follows:

F:

$$p_{-1} = 2.0; \qquad p_k = (k+2)/(k-1) \quad \text{for } k > 1; \qquad \lim_{k\to\infty} p_k = 1 \tag{21}$$

LN:

$$p_k = b \text{ for all } k; \qquad \lim_{k\to\infty} p_k = b$$
$$\text{for some constant } b > 1 \tag{22}$$

Table I shows our computed R-equivalent Δ-function distributions obtained by matching the moments $\{M_R^{(0)}\}$ (eq 3) with those of F or LN reference distributions (eq 21 and 22) in each case with the normalized ($M_0 = 1$) moment $M_1 = 2.0 \times 10^5$ and $p_1 = 1.5$. We draw attention to the appearance of trace amounts of a very high molecular weight component in the LN case. This feature was found by Šolc[16] to have a profound influence on the dilute-solution branch of the CPC (see below and also Figure 2).

Obviously, an R-equivalent distribution, like any other MWD, implies moments $M_{k(\text{eqt})}$ of all orders although, except for R of them, these moments will not be identical with those of the reference distribution, $M_{k(\text{ref})}$. This suggests an assessment of the effects of truncation based on a comparison of unmatched moments. For this purpose we define the following factors:

$$f_k \equiv 1 - (M_{k(\text{eqt})}/M_{k(\text{ref})}); \qquad k = 0, 1, \ldots \tag{23}$$

For a Δ-function distribution which is R-equivalent in the R integral order moments of the set $\{M_R^{(0)}\}$, clearly $f_k = 0$ for $k = 0, 1, \ldots, R-1$. Furthermore, because the reference distribution will always include species of higher molecular weight than *any* R-equivalent distribution, $0 \le f_k < 1$ for all k. In Table II we give numerical results for f_k, $k = R, R+1, R+2$, for the R-equivalent distributions detailed in Table I. These factors, f_k, are significantly smaller in the case of F reference distributions than for LN distributions, a fact that has significance in the rate of convergence of R-equivalent computations of phase loci (see below).

Table II
Numerical Values of the Factors f_k (Eq 23) for the R-Equivalent Distributions of Table I

R	MWD	f_R	f_{R+1}	f_{R+2}
2	F	0.6667	0.9167	0.9833
	LN	0.6667	0.9293	0.9890
4	F	0.1000	0.3000	0.5286
	LN	0.1852	0.5281	0.8147
6	F	0.0286	0.1142	0.2571
	LN	0.1339	0.4386	0.7482
8	F	0.0078	0.0398	0.1093
	LN	0.1011	0.3818	0.7016

In keeping with the spirit of R-equivalence, we prefer to rewrite eq 5 and 6 in the form, using moments scaled so that $M_0 = \phi$,

$$\Delta G^+ = (1 - M_0)\ln(1 - M_0) + \sum_i \phi_i c m_i^{-1} \ln \phi_i + \Gamma \tag{24}$$

where

$$\Gamma = M_0(1 - M_0)g$$
$$M_0 \equiv \sum_i \phi_i \tag{25}$$

In this form, our choice of two ΔG functions, referred to hereafter as GI and GII, is

GI: Flory–Huggins[10,11]

$$\Gamma = \Gamma(M_0, T)$$
$$g = T_\Theta/2T \tag{26}$$

where T_Θ is the Θ temperature.

GII:
Koningsveld, Stockmayer, Kennedy, and Kleintjens[17]

$$\Gamma = \Gamma(M_0, M_1, T)$$
$$g = (\beta_0 + \beta_1/T)/(1 - \gamma M_0) + g^* \exp(-\lambda_0(M_0M_1)^{1/2}) \tag{27}$$

where β_0, β_1, γ, and λ_0 are adustable parameters and g^* is defined by

$$g^* = (0.5 - (\beta_0 + \beta_1/T)(1 - \gamma))(1 - h(z))/(1 + \lambda_0(M_1/M_0)^{1/2}) \tag{28}$$

In GII we use the Casassa–Markovitz form of the function $h(z)$, which arises in dilute-solution theory,[18] since this form is free from singularities when $z < 0$; that is, $T < T_\Theta$. Thus

$$h(z) = (1 - \exp(-5.73z))/(5.73z) \tag{29}$$

where

$$z = 0.305(0.5 - (\beta_0 + \beta_1/T)(1 - \gamma))(M_1/M_0)^{1/2} \tag{30}$$

We apply our computational methods to the system polystyrene/cyclohexane, for which

$$c = 117.76; \qquad T_\Theta = 306.0 \text{ K} \tag{31}$$

and the parameters of GII, found by optimization of spinodal data, are[19]

$$\beta_0 = 0.3832 \qquad \beta_1 = 108.59 \text{ K}^{-1}$$
$$\gamma = 0.3251 \qquad \lambda_0 = 0.57 \tag{32}$$

3.1. Spinodal and Critical Loci

Because out two ΔG functions (eq 26 and 27) each have an interaction term that depends on a finite set of moments, it follows (eq 8 and 9) that the corresponding

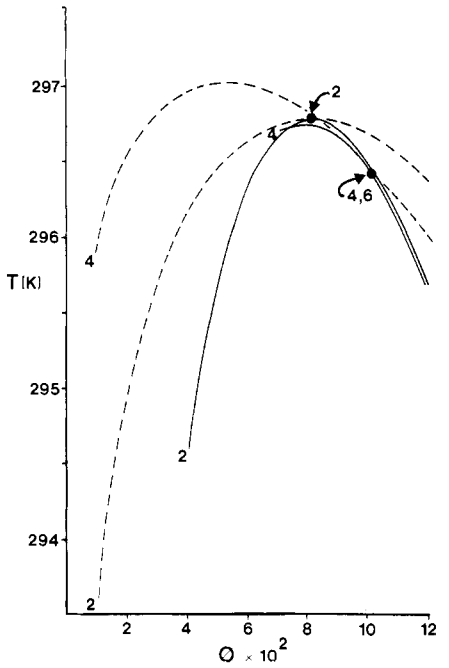

Figure 1. Spinodals (solid lines) and critical points (filled circles) for R-equivalent Δ-function distributions with moments $\{M_R^{(0)}\}$ constrained to match those of a Flory distribution normalized with $M_1 = 2.0 \times 10^5$. Calculations were performed with ΔG function GII (eq 34) and the numbers indicate values of R used to obtain the curve. E.g., $R = 4$ indicates that the moments $\{M_0, M_1, M_2, M_3\}$ are matched to those of the reference distribution. Also drawn are the corresponding CPC loci (dashed lines); cf. Figure 2.

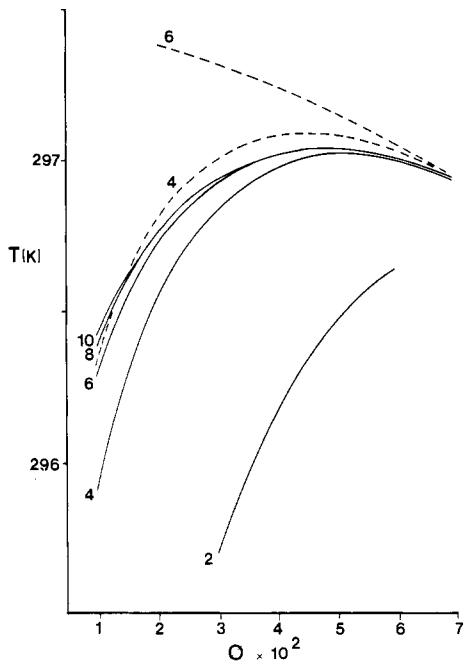

Figure 2. Subcritical CPC branches calculated using ΔG function GII for R-equivalent Δ-function distributions with $\{M_R^{(0)}\}$ matching moments of reference F (solid lines) and LN (dashed lines) distributions. For both reference distributions the critical points almost conincide, $\phi_{cr} \cong 0.10$ (cf. Figure 1). Notice how each set of curves "fans out" toward lower concentrations, though much more strongly in the case of LN than F. This feature was already foreshaddowed in part by Table II.

spinodal and critical point temperatures also depend on finite sets of moments; thus

$$\text{GI:} \quad \Gamma = \Gamma(M_0) \quad \therefore \quad \begin{aligned} T_{sp} &= T_{sp}(M_0, M_1) \\ T_{cr} &= T_{cr}(M_0, M_1, M_2) \end{aligned} \tag{33}$$

$$\text{GII:} \quad \Gamma = \Gamma(M_0, M_1) \quad \therefore \quad \begin{aligned} T_{sp} &= T_{sp}(M_0, M_1, M_2, M_3) \\ T_{cr} &= T_{cr}(M_0, M_1, M_2, M_3, M_4, M_5) \end{aligned} \tag{34}$$

Spinodals and critical points computed by the methods outlined in part 2 for the ΔG function GII are shown in Figure 1. In these examples the set of R-equivalent moments $\{M_R^{(0)}\}$ (cf. eq 3) has been constrained to obey a Flory MWD (eq 21) with $M_1 = 2.0 \times 10^5$. With $R = 2$, the moments M_0 and M_1 are matched to those of the reference F distribution. The R-equivalent Δ-function distribution then contains only one component, and, as is well-known, the critical point appears at the spinodal maximum. The nature of the R-equivalent Δ-function distribution is such that we are forced to increase the order of $\{M_R^{(0)}\}$, and hence the number of matched moments, by *two* at a time in spite of the fact that, for GII, the spinodal temperature is invariant to moments of order R ≥ 3. This is not so for the critical point until $R \geq 6$; however, calculated critical points for $R = 4$ and $R = 6$ practically coincide. There are two reasons for this: First, the moments M_4 and M_5 for the 4-equivalent Δ-function distribution, although not matched to those for the reference F distribution, do not differ strongly from the reference moments (cf. Table II). Second, even when the critical point exhibits a formal dependence on higher moments (e.g., M_4 and M_5 as in eq 34), its sensitivity to M_k diminishes with increasing k as has been observed elsewhere.[8]

3.2. Cloud Point Curves

As previously mentioned we know of no exact-truncation result for the moment expansion of a CPC, nor indeed do we believe any such result is likely. This is borne out by the subcritical (i.e., usually $\phi < \phi_{cr}$) branches of CPC's calculated for ΔG function GII and shown in Figure 2. The R-equivalent Δ-function distributions have moments $\{M_R^{(0)}\}$ constrained to match either F or LN reference distributions normalized with $M_1 = 2.0 \times 10^5$ and $p_1 = 1.5$.

The critical concentrations for these reference F and LN distributions (or for their R-equivalent Δ-function distributions when $R \geq 6$, eq 34) are almost identical ($\phi_{cr} \simeq 0.10$). There is a striking difference, however, in CPC behavior as R increases, made obvious (Figure 2) by the way the two sets of curves "fan out" at progressively lower concentrations (cf. ref 20). Denote by $T_{cl}(\{M_R^{(0)}\})_\phi$ the cloud point temperature at fixed ϕ of the R-equivalent Δ-function distribution with $\{M_R^{(0)}\}$ moments matched to those of the reference distribution. Then, as our calculations show (see Figure 2), for both F and LN reference distributions, $|T_{cl}(\{M_{R+2}^{(0)}\})_\phi - T_{cl}(\{M_R^{(0)}\})_\phi|$ *increases as* ϕ *decreases and decreases as* R *increases.*

Apparently, the location of the subcritical branch of a CPC is increasingly influenced by progressively higher moments of a MWD (i.e., by higher molecular weight components) on moving away from a critical point. On the other hand, convergence in R-equivalent CPC computations is suggested, at least qualitatively, by the decreasing effect of incrementing R. This effect is much more rapid with an F reference MWD than it is with LN, as might have been anticipated by the differences in the factors f_k ($k > R$) noted above for F and LN distributions (see Table II).

Our assessment of R-equivalent CPC computations is hampered by the difficulty in extrapolating to the result $T_{cl}(\{M_\infty^{(s)}\})$ for the Δ-function distribution in which all moments match those of the reference MWD. We have investigated this convergence problem by comparing our calculations with those of Koningsveld[21] and based on direct use of a *continuous* MWD function truncated at

Table III
Cloud Point Temperatures (K) for Δ-Function Distributions R-Equivalent to an F Distribution, Using ΔG Function GI, Compared with Results of Koningsveld[21] Based on a Truncated Continuous MWD

vol fraction $\phi \times 10^3$	no. of moments matched R				Koningsveld
	4	6	8	10	
2.5	286.04			288.65	
5.0	287.72	289.01	289.28	289.35	289.33
7.5	288.58	289.50	289.66	289.69	289.66
10.0	289.09	289.76	289.85	289.86	289.88
12.5	289.39	289.87	289.93	289.93	289.94
15.0	289.55	289.90	289.93	289.93	289.94
17.5		289.86		289.87	289.88

finite molecular weight m_{max} (=1.5 × 10⁷). For this set of calculations we have used the ΔG function GI (eq 26) with R-equivalent Δ-function distributions having moments $\{M_R^{(-1)}\}$ matched to those of F or LN reference distributions.

For the F distribution (eq 21, normalized with M_1 = 1.317 × 10⁵ and p_{-1} = 2.0) we find (see Table III) at all concentrations excellent agreement between our calculations ($R \geq 8$) and those of Koningsveld[21] estimated graphically from the original source to within ±0.05 K. The critical concentration, which depends only on (M_0, M_1, M_2) (eq 33) and is thus invariant for $R \geq 4$, lies at ϕ_{cr} = 0.034.

Analogous results for a LN distribution (eq 22, with M_1 = 1.317 × 10⁵ and p_k = 2.0) are presented in Table IV. In this case accurate computation becomes difficult as R increases and we have omitted from Table IV R-equivalent CPC temperatures for which convergence is slow. The difficulty is associated with the appearance of trace amounts of a very high molecular weight component (cf. Table I). Though its effect can be minimized through use of high-precision computational techniques, we have not done so here since our main purpose is to illustrate R-equivalence. For comparison with Koningsveld's calculations, we note that the highest molecular weight component of our 10-equivalent Δ-function distribution has w = 6.46 × 10⁻¹⁰ and m = 2.46 × 10⁷.

For ΔG function GI and LN distributions, Šolc[16] showed that the subcritical branch of a CPC is *independent* of the common molecular weight averages $\bar{M}_{-1}$, $\bar{M}_1$, $\bar{M}_2$, etc. and obeys the simple relation

$$T_{cl}(\phi) = T_\Theta(1 - \phi)$$
$$T_\Theta = \lim_{m \to \infty} T_{cr} \tag{35}$$

According to Šolc, this unusual behavior, the CPC showing a maximum $T_{cl} = T_\Theta$ at $\phi_{cl} = 0$, results from the presence of infinitesimal but significant amounts of material with $m \to \infty$. This is the obvious reason for the large differences obtained in calculated values of T_{cl} shown in Table IV. For example, in the Koningsveld calculation there is complete exclusion of all species with $m > m_{max}$. Another view of our results is provided by a Taylor expansion to first order in moments of the difference $\Delta T_{cl}(R,\phi)$ between cloud point temperatures of R-equivalent and reference (equally, ∞-equivalent) distributions. Thus

$$\begin{aligned}\Delta T_{cl}(R,\phi) &\equiv T_{cl}(\{M_R^{(s)}\})_\phi - T_{cl}(\{M_\infty^{(s)}\})_\phi \\ &= \sum_{k \geq s} C_k f_k M_{k(\text{ref})} \\ &= \sum_{k \geq (R+s)} C_k f_k M_{k(\text{ref})}\end{aligned} \tag{36}$$

where C_k is a constant associated with the kth moment contribution to T_{cl}, f_k is as defined in eq 23, and the final equality follows from the definition (eq 3) of R-equivalent Δ-function distributions. Clearly, the magnitude of $\Delta T_{cl}(R,\phi)$ depends directly on the factors f_k which relate to moments (of order $k > R + s$) not matched to those of the reference MWD. These factors depend markedly on the form of the reference distribution (see Table II). In general, the broader the distribution, the more moments that must be matched to construct R-equivalent distributions for which acceptable (i.e., small enough ΔT_{cl}) cloud point temperatures can be computed.

Coexisting phase composition data, determined by our R-equivalent CPC computations (Tables III and IV), are given in Table V in terms of volume fractions, molecular

Table IV
Cloud Point Temperatures (K) for Δ-Function Distributions R-Equivalent to an LN Distribution, Using ΔG Function GI, Compared with Results of Koningsveld[21] and Analytic Results of Šolc[16] for This Case (Compare with Table III)

vol fraction $\phi \times 10^3$	no. of moments matched R				Koningsveld	Šolc eq 35
	4	6	8	10		
5.0	289.85	293.85	297.00		293.44	304.47
7.5	290.36	293.60			293.38	303.71
10.0	290.60	293.26	295.81		293.10	302.94
12.5	290.67	292.87	295.19		292.88	302.18
15.0	290.64	292.44	294.55	296.76	292.43	301.41
17.5		291.99	293.91		291.98	300.65

Table V
Volume Fractions, Molecular Weight Averages, and Polydispersity Indices p_k (Eq 20) of the Incipient (Conjugate) Phase from the CPC Computations of Table III (F Distribution) and Table IV (LN Distribution) and Analytic Predictions of Solc[22]

R	MWD	vol fractions					mol wt averages × 10⁻⁵				
		ϕ_1	ϕ_2	ϕ_3	ϕ_4	ϕ_5	$\bar{M}_{-1}$	$\bar{M}_1$	$\bar{M}_2$	p_{-1}	p_1
4	F	0.0382	0.0099				1.128	1.865	2.168	1.653	1.162
	LN	0.0335	0.0147				1.238	2.550	3.271	2.060	1.283
6	F	0.0173	0.0273	0.0054			1.191	2.288	3.143	1.921	1.374
	LN	0.0226	0.0162	0.0112			1.543	7.893	13.78	5.155	1.746
8	F	0.0055	0.0208	0.0207	0.0034		1.204	2.395	3.510	1.989	1.466
	LN	0.0244	0.0013	0.0102	0.0095		1.689	35.61	62.90	21.08	1.766
10	F	0.0014	0.0096	0.0210	0.0161	0.0023	1.210	2.412	3.601	1.993	1.493
	LN	0.0197	10^{-4}	0.0004	0.0079	0.0087	1.509	142.4	262.7	94.37	1.845
Šolc	F									2.000	1.500
	LN									(∞)	

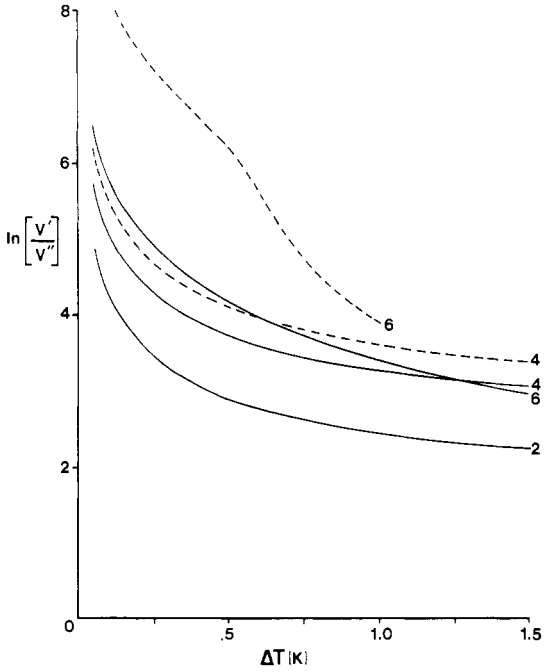

Figure 3. Logarithm of phase volume ratio (Q) (eq 17) computed for R-equivalent Δ-function distributions (as under Figure 2) at an overall polymer concentration $\phi = 0.03$. Q is plotted as a function of $\Delta T \equiv T_{cl} - T$. Reference MWD is F (solid lines) or LN (dashed lines) and numbers are values for R.

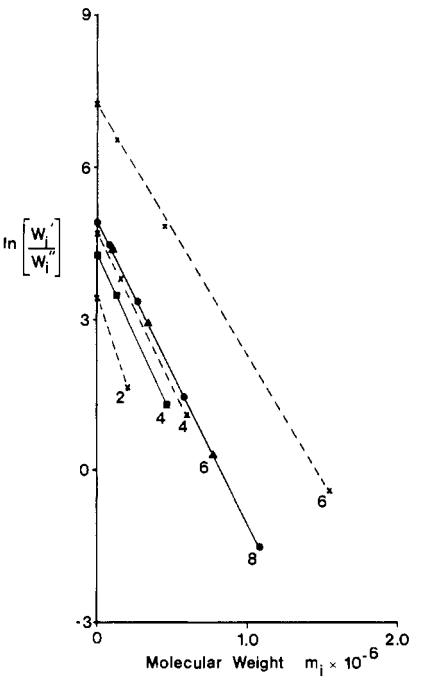

Figure 4. B–W plots (eq 16) obtained at $\phi = 0.03$ and $\Delta T = 0.25$ K for the R-equivalent Δ-function distributions in Figures 2 and 3. Symbols locate computed values for partition coefficients of individual Δ-function components as detailed in Table I.

weight averages, and polydispersity indices p_k (eq 20) for the incipient (conjugate) phase. Of especial interest are the polydispersity indices sine these offer a quantitative measure of the extent of polymer fractionation.

Again, for the ΔG function GI, Šolc has obtained analytic results.[22] He concludes that for any F distribution (e.g., as in Table III), the limiting (incipient phase separation) conjugate phase polydispersity is identical with that in the principal phase; that is, $p_k' = p_k''$ ($k = -1, 1, ..., \infty$). However, for *any* LN distribution (as in Table IV), $p_{-1}'' = \infty$. Our calculations (Table V) show general agreement with these predications. However, just as in our CPC calculations, the rate of convergence (with increasing R) on the results of Šolc is much faster with an F reference distribution than with an LN distribution.

3.3. Phase Volume Ratios and B–W Plots

Figures 3 and 4 illustrate phase volume ratios and B–W plots computed for an overal polymer concentation $\phi = 0.03$ using the methods outlined in section 2.2.3. We have produced these using ΔG function GII and R-equivalent Δ-function distributions with moments $\{M_R^{(0)}\}$ matched to either F or LN reference distributions normalized with $M_1 = 2.0 \times 10^5$ and $p_1 = 1.5$. We have not investigated convergence with R for these loci, but the trends are expected to be similar to our CPC computations since all are governed by the same thermodynamic requirement, namely, eq 12. We do, indeed, note that similar difference in behavior occur for the two types of reference distributions. A feature that deserves mention is that our B–W plots are slightly concave, more pronounced for the LN reference distribution. This is characteristic of the ΔG function GII as first reported by Kleintjens et al.,[23] who employed Koningsveld's method of computation.

4. Discussion

The mathematical problem of specifying a probability distribution function (pdf) from a finite set of its moments is well documented (see, for example, Shohat and Tamarkind[24] and Collins and Wragg[25]). Similarly, the expression of polymer properties as expansions in terms of the moments of its MWD is not uncommon in practice (cf. Flory[26]). The present work embraces both of these ideas, albeit in slightly different form since (i) the specified pdf is finite and unique and (ii) in contrast to common moment expansions, here all moments are taken account of but only some of them are accounted for exactly. A theoretical examination of the Gibbs criteria for phase equilibria in polydisperse polymer solutions indicates that we may expect *exact* truncation after finitely many moments in some such expansions. More generally, however, complete knowledge of the MWD is necessary for exact computation although, for many purposes, the truncated expansion may be expected to converge on the exact result as more moments are specified exactly. In these cases our recipe for producing Δ-function distributions with moments from a suitable set (such as those of positive integral orders) matched to those of some reference MWD is convenient and general. It is applicable to *any* ΔG function. A similar approach seems suitable for modeling other properties such as the distribution of relaxation times in the computation of viscoelastic phenomena (cf. Shen[27]). Analogous to truncation of moment expansions proved for spinodal and critical point loci when appropriate theoretical ΔG functions are involved, similar conclusions are implied by the extended Rouse–Bueche theory[28] for zero-shear viscosity and the elastic steady-state compliance of polydisperse polymer melts and solutions.

Acknowledgment. P.A.I. thanks the Department of Chemistry, University of Essex, for a studentship. J.W.K. acknowledges financial support from the Science Research Council (U.K.) while at the University of Essex and Baruch College of the City University of New York for their hospitality and help during 1980–1981. We thank M. Gordon and J. A. Torkington (Essex) for their suggestions and help with some of the calculations and R. Koningsveld (DSM) for communication of his results prior to publication. We are especially appreciative of the useful comments offered by one of the referees.

Appendix 1. Numerical Solution of Moment Equations

An R-equivalent Δ-function distribution comprises $R^* \equiv [R/2]$ components whose weight fractions and molecular weights are uniquely specified (see Appendix 2) as the solution $\{w_{\mathbf{R}^*}, m_{\mathbf{R}^*}\}$ to the system of R simultaneous nonlinear equations

$$\sum_{i=1}^{R^*} w_i m_i^k = M_k; \qquad k = s, s+1, ..., R+s-1 \tag{A1-1}$$

The numerical solution of these equations is straightforward[9] and we summarize our implementation of the method in three steps:

Step 1

Let $\{m_{\mathbf{R}^*}\} \equiv \{m_j; j = 1, 2, ..., R^*\}$ be the set of zeros of the polynomial $Q(m)$:

$$Q(m) \equiv \sum_{j=0}^{R^*} \alpha_{R^*-j} m^{j+s}; \qquad \alpha_0 = 1 \tag{A1-2}$$

Define matrices $\tilde{H}$, $\tilde{A}$, and $\tilde{X}$ thus:

$$\tilde{H}_{(R^*\times R^*)} \equiv [H_{uv} = M_{u+v+s-2}; \qquad u, v = 1, 2, ..., R^*] \tag{A1-3}$$

$$\tilde{A}_{(R^*\times 1)} \equiv [A_u = -M_{R^*+s+u-1}; \qquad u = 1, ..., R^*] \tag{A1-4}$$

$$\tilde{X}_{(R^*\times 1)} \equiv [X_u = M_{R^*+1-u}; \qquad u = 1, ..., R^*] \tag{A1-5}$$

The first step then involves solving the linear matrix equation

$$\tilde{H}\tilde{X} = \tilde{A} \tag{A1-6}$$

for the unknown vector $\tilde{X}$. For this we have used standard software,[29] NAG subroutine F04AAF.

Step 2

The unknown molecular weights $\{m_{\mathbf{R}^*}\}$ are determined as roots of the polynomial $Q(m)$ (eq A1-2), whose coefficients α_{R^*-j} are the elements of vector $\tilde{X}$ found in step 1. For step 2 we have used the polynomial root-finding subroutine NAG:C02AAF.[29]

Step 3

Analogous to eq A1-3 to A1-5 define matrices $\tilde{B}$, $\tilde{C}$, and $\tilde{D}$ thus:

$$\tilde{B}_{(R^*\times R^*)} \equiv [B_{uv} = m_v{}^{u+s-1}; \qquad u, v = 1, ..., R^*] \tag{A1-7}$$

$$\tilde{C}_{(R^*\times 1)} \equiv [C_u = w_u; \qquad u = 1, ..., R^*] \tag{A1-8}$$

$$\tilde{D}_{(R^*\times 1)} \equiv [D_u = M_{u+s-1}; \qquad u = 1, ..., R^*] \tag{A1-9}$$

where the elements of $\tilde{B}$ are members of the set $\{m_{\mathbf{R}^*}\}$ found in step 2. The set of weights $\{w_{\mathbf{R}^*}\}$ (or weight fractions if $M_0 = 1$) are obtained by solving the matrix equation

$$\tilde{B}\tilde{C} = \tilde{D} \tag{A1-10}$$

for the unknown vector $\tilde{C}$ (NAG:F04AAF[29]).

The sets $\{w_{\mathbf{R}^*}\}$ and $\{m_{\mathbf{R}^*}\}$ together comprise the requisite solution $\{w_{\mathbf{R}^*}, m_{\mathbf{R}^*}\}^{(s)}$. Throughout this paper we have used two cases: $s = 0$ and $s = -1$.

Appendix 2. Uniqueness of Solutions to Moment Equations

We first restate the problem in the form used by Steiltjes[24] for the positive axis $0 < m < \infty$. For even $\mathbf{R}$, a given moment set $\{M_{\mathbf{R}}{}^{(0)}\} \equiv \{M_0, M_1, ..., M_{R^{-1}}\}$, that is, a sequence of real numbers, it is required to determine positive numbers

$$w_1 > 0, w_2 > 0, ..., w_{R^*} > 0$$
$$m_1 > m_2 > ... \mu_{R^*} > 0 \tag{A2-1}$$

subject to the conditions in eq A1-1. (Of course, if $\mathbf{R}$ is odd, then the simple stratagum of supplying *any* value for the $R+1$ moment changes the problem to that for even $\mathbf{R}$.) We state, without giving a proof here, the following:

Theorem (Shohat and Tamarkind[24] and Gantmacher[30])

The finite problem of moments (finite even R) has a unique solution if and only if

$$D_0 > 0, D_1 > 0, ..., D_{R^*-1} > 0$$
$$D_0{}^* > 0, D_1{}^* > 0, ..., D_{R^*-1}{}^* > 0 \tag{A2-2}$$

where the D_k are Hankel determinants (persymmetrics) of the moments; viz.

$$D_k = \begin{vmatrix} M_0 & M_1 & \cdots & M_k \\ M_1 & M_2 & \cdots & M_{k+1} \\ & \cdots\cdots & & \\ M_k & M_{k+1} & \cdots & M_{2k} \end{vmatrix}$$

$$D_k^* = \begin{vmatrix} M_1 & M_2 & \cdots & M_{k+1} \\ M_2 & M_3 & \cdots & M_{k+2} \\ & \cdots\cdots & & \\ M_{k+1} & M_{k+2} & \cdots & M_{2k+1} \end{vmatrix} \tag{A2-3}$$

We now demonstrate uniqueness of solutions to the moment equations for Flory (F) and log-normal (LN) molecular weight distributions (eq 21 and 22) by showing that the Hankel determinants for these distributions are all positive. Thus:

Theorem A2.1

A normalized (Flory) molecular weight distribution with moments

$$M_0 = 1$$
$$M_k = (k+1)!(M_1/2)^k$$

has positive Hankel determinants (persymmetrics).

Proof

There are two cases.

(1) The kth even persymmetric for the F distribution is

$$\begin{aligned} D_k &= \det [M_{(i+j-2)}; \qquad i, j = 1, k+1] \\ &= \det [(i+j-1)!(M_1/2)^{i+j-2}; \qquad i, j = 1, k+1] \\ &= (M_1/2)^{\omega} \det [(i+j-1)!; \qquad i, j = 1, k+1] \end{aligned}$$

where $\omega = 2 + 4 + 6 + ... + 2k = k(k+1)$, since in the expansion of D_k each of the terms contains the constant factor $(M_1/2)^{\omega}$.

Dividing the ith row of the determinant by $i!$ and the jth column by $(j-1)!$, we obtain

$$D_k = (M_1/2)^{k(k+1)} \prod_{l=1}^{k} l!(l-1)! X_k$$

where

$$X_k = \det \left[\frac{(i+j-1)!}{i!(j-1)!} = \binom{i+j-1}{i}; \qquad i, j = 1, k+1 \right]$$

is a determinant of binomial coefficients that can be re-

duced to triangular form with unit diagonal elements by repeated row subtractions; i.e., subtract row 1 from rows 2, 3, ..., $k+1$, then row 2 from rows 3, 4, ..., $k+1$, etc.

Consequently, $X_k = 1$ and thus

$$D_k = (M_1/2)^{k(k+1)} \prod_{l=1}^{k} l!(l-1)! > 0$$

(2) Similarly, for the kth odd persymmetric of the F distribution

$$\begin{aligned} D_k^* &= \det [M_{(i+j-1)}; \quad i,j = 1, k+1] \\ &= \det [(i+j)!(M_1/2)^{i+j-1}; \quad i,j = 1, k+1] \\ &= (M_1/2)^{\nu} \det [(i+j)!; \quad i,j = 1, k+1] \end{aligned}$$

where $\nu = 1 + 3 + 5 + \ldots + (2k+1) = (k+1)^2$.

Dividing the ith row by $(i+1)!$ and the jth column by $(j-1)!$, we obtain

$$D_k^* = (M_1/2)^{\nu} \prod_{l=1}^{k+1} (l+1)!(l-1)! \det \left[\binom{i+j}{i+1}; \quad i,j = 1, k+1 \right]$$

where again the determinant can be reduced to unit triangular form by repeated row subtractions as with X_k above. Hence

$$D_k^* = (M_1/2)^{(k+1)^2} \prod_{l=1}^{k+1} (l+1)!(l-1)! > 0$$

Theorem A2.2

A normalized (LN) molecular weight distribution with moments

$$M_0 = 1$$

$$M_k = b^{k(k-1)/2} {M_1}^k$$

for some constant $b > 1$ has positive Hankel determinants.

Proof (Compare with Theorem A2.1)

For the kth even persymmetric of the LN distribution

$$\begin{aligned} D_k &= \det [M_{(i+j-2)}; \quad i,j = 1, k+1] \\ &= \det [b^{(i+j-2)(i+j-3)/2} {M_1}^{(i+j-2)}; \quad i,j = 1, k+1] \\ &= {M_1}^{k(k+1)} \det [b^{(i+j-2)(i+j-3)/2}; \quad i,j = 1, k+1] \end{aligned}$$

Dividing the ith row of the determinant by $b^{(i-1)(i-2)/2}$ and the jth column by $b^{(j-1)(j-2)/2}$ yields

$$D_k = {M_1}^{k(k+1)} \prod_{l=1}^{k+1} b^{(l-1)(l-2)} Y_k$$

where

$$Y_k = \det [b^{(i-1)(j-1)}; \quad i,j = 1, k+1]$$

Subtract row k from row $(k+1)$, then subtract row $(k-1)$ from row k, etc.:

$$\begin{aligned} \therefore \quad Y_k &= \det [b^{(i-1)(j-1)}(b^{j-1} - 1); \quad i,j = 2, k+1] \\ &= \prod_{l=1}^{k} b^{l-1}(b^l - 1) \det [b^{(i-1)(j-1)}; \quad i,j = 1, k] \\ &= \prod_{l=1}^{k} b^{l-1}(b^l - 1) Y_{k-1} \end{aligned}$$

Since $Y_0 = 1$, we have, finally, from this recursive result that

$$Y_k = \prod_{m=1}^{k} \prod_{l=1}^{m} b^{l-1}(b^l - 1)$$

Hence

$$D_k = {M_1}^{k(k+1)} \prod_{l=1}^{k+1} b^{(l-1)(l-2)} \prod_{m=1}^{k} \prod_{l=1}^{m} b^{l-1}(b^l - 1) > 0$$

as was required to be proved.

For the kth odd persymmetric

$$\begin{aligned} D_k^* &= \det [M_{(i+j-1)}; \quad i,j = 1, k+1] \\ &= \det [b^{(i+j-1)(i+j-2)/2} {M_1}^{(i+j-2)}; \quad i,j = 1, k+1] \\ &= {M_1}^{\nu} \prod_{l=1}^{k+1} b^{l-1} \det [b^{(i-1)(j-1)}; \quad i,j = 1, k+1] \\ &= {M_1}^{\nu} \prod_{l=1}^{k+1} b^{l-1} Y_k \\ &= {M_1}^{\nu} \prod_{l=1}^{k+1} b^{l-1} \prod_{m=1}^{k} \prod_{l=1}^{m} b^{l-1}(b^l - 1) < 0 \end{aligned}$$

where $\nu = (k+1)^2$.

Appendix 3. Computation of Spinodal and Critical Loci

Our R-equivalent spinodal calculation, at fixed ϕ, requires finding the temperature T_{sp} for which the smallest eigenvalue λ_0 of the spinodal matrix (eq 10) J_1 takes the value zero. After constructing J_1 from an explicit expression for the derivatives $\partial^2 \Delta G / \partial \phi_i \partial \phi_j$; $i,j = 1, \ldots, R^*$ (cf. eq 7), we use NAG:E02AGF[29] to find the R^* eigenvalues and eigenvectors of J_1 from which λ_0 is located. By stepwise variation of temperature T we search for an interval ΔT (usually 2.5 K) within which λ_0 changes sign and then employ a bisection method to reduce the interval ΔT ($\equiv T_1 - T_2$) to about 10^{-4} K. The spinodal temperature $T_{sp}(\phi) = (T_1 + T_2)/2$ and typically $\lambda_0(T_1) \simeq \lambda_0(T_2) \simeq 10^{-6}$–$10^{-8}$.

For each spinodal point (ϕ_{sp}, T_{sp}) the vector $\tilde{\phi}_{sp} \equiv \{\phi_{1,sp}, \ldots, \phi_{R^*,sp}\}$ is fully determined by ϕ_{sp} and the R-equivalent weight distribution. At each such point NAG:E02AGF[29] also finds $\tilde{\xi}_0$, the normalized (i.e., $\tilde{\xi}_0 \cdot \tilde{\xi}_0 = 1$) eigenfunction associated with λ_0 (=0). To determine if a spinodal point is also critical, we compute $\lambda_0^{(d)}$, the smallest eigenvalue of $\tilde{J}_1$ at a point $\tilde{\phi}_{sp} + d\tilde{\xi}_0$ in composition space a small distance d along the eigenvector from $(\tilde{\phi}_{sp}, T_{sp})$. Similarly, we evaluate $\tilde{\xi}_0^{(-d)}$, the smallest eigenvalue of $\tilde{J}_1$ at a point $\tilde{\phi}_{sp} - d\tilde{\xi}_0$. The difference $\Delta\lambda_0^{(d)} \equiv \lambda_0^{(d)} - \lambda_0^{(-d)}$ is a direct measure of the scalar quantity $\tilde{\nabla} J_1 \cdot \tilde{\xi}_0$ that takes zero value at a critical point.

For fixed $d \simeq 10^{-3}$ we locate three spinodal points covering a range in which $\Delta\lambda_0^{(d)}$ changes sign. For all purposes considered in this paper, a quadratic fit to these points was adequate to locate $\phi_{cr,d}$, an estimate for the volume fraction at which $\Delta\lambda_0^{(d)} = 0$.

Strictly, $\tilde{\nabla} J_1 \cdot \tilde{\xi}_0$ is only directly proportional to $\Delta\lambda_0^{(d)}$ in the limit $d \to 0$. Thus, the above procedure can be repeated with smaller step length d followed by extrapolation to locate $\phi_{cr} = \phi_{cr,d=0}$. Certainly, a linear extrapolation will suffice, though in practice this is usually unnecessary.

With the critical concentration ϕ_{cr} located, T_{cr} is found using the spinodal routine as above, with $\phi = \phi_{cr}$.

Appendix 4. Computation of CPC and Associated Features

CPC, phase volume ratio, and B–W plots all involve finding conditions under which a set of chemical potentials has equal values in two phases (see eq 12). For an R-equivalent Δ-function distribution this necessitates minimization of the quantity S

$$S \equiv \sum_{i=0}^{R^*} (\Delta\mu_i' - \Delta\mu_i'')^2 \qquad \text{(A4-1)}$$

for which purpose we use a double-precision version of a nonlinear equation root-finding subroutine, NAG: C05NAF,[29] with algebraic expressions for $\Delta\mu_i'$ and $\Delta\mu_i''$

separately provided. For our CPC calculations S is minimized with respect to $\{\tilde{T}, \sigma_1, \sigma_2, ..., \sigma_{R^*}\}$, where

$$\sigma_i \equiv \ln (\phi_i''/\phi_i')/m_i \qquad \text{(A4-2)}$$

and $\tilde{T} = \tilde{T}/T^*$, where T^* is a constant scale factor chosen so that $\tilde{T}$ has about the same magnitude as σ. The algorithm NAG:C05NAF, which has to evaluate elements of the Jacobian matrix of $(\Delta\mu' - \Delta\mu'')^2$, performs best when its arguments are of similar magnitude.

For B-W plot and phase volume ratio calculations S is minimized with respect to $\{\sigma_1, \sigma_2, ..., \sigma_R^*\}$, since here T is fixed.

Before NAG:C05NAF is called a preliminary search is performed with respect to σ (or σ and $\tilde{T}$) to locate a minimum in S, using $\sigma_i = \sigma'$ for all i. This condition on the σ_i is, in fact, the case for ΔG function GI (eq 26) for which σ depends only on ϕ, though not for GII (eq 27), where $\sigma_i = \sigma_i(m_i)$. Once this approximate solution $(\sigma', \tilde{T}')$ is found, artificial bounds $\Delta\sigma$ and ΔT are placed on the arguments, viz.: $(\sigma' - \Delta\sigma) < \sigma_i < (\sigma' + \Delta\sigma)$ and $(\tilde{T}' - \Delta T) < \tilde{T} < (\tilde{T} + \Delta T)$ so that the program is confined to work over a limited range in σ/T space, with S being set to a very large value if an iteration results in a root being "out of bounds".

For the calculations presented in this paper true roots were usually obtained with $S < 10^{-16}$, with cloud point temperatures accurate to $\pm 5 \times 10^{-4}$ K and with phase compositions accurate to $\pm 10^{-4}$.

A tricky feature of these calculations is to avoid the trivial roots $\sigma_i = 0$. This problem becomes more pronounced near a critical point, where the two phases become identical. We did not pursue these calculations, but one possibility is to divide out the trivial root and minimize $S = \sum_i(\Delta\mu_i' - \Delta\mu_i'')^2/\sigma_i$; but now the convergence criteria must be chosen with care since when σ is small, S may become rather large.

References and Notes

(1) Koningsveld, R.; Staverman, A. J. *J. Polym. Sci., Part A-2* **1968**, *6*, 305, 325, 349.
(2) Gibbs, J. W. *Trans. Conn. Acad. Arts Sci.* **1878**, *3*, 108, 343 (reprinted in: "The Scientific Papers of J. W. Gibbs"; Dover Publications: New York, 1961; Vol. 1).
(3) Derham, K. W.; Goldsborough, J.; Gordon, M. *Pure Appl. Chem.* **1974**, *38*, 97.
(4) Kennedy, J. W. *Spec. Period. Rep.: Macromol. Chem.* **1979**, *1*, Chapter 14.
(5) Irvine, P.; Gordon, M. *Macromolecules* **1980**, *13*, 761.
(6) Gordon, M.; Irvine, P.; Kennedy, J. W. *J. Polym. Sci., Polym. Symp.* **1977**, *No. 61*, 199.
(7) Irvine, P.; Gordon, M. *Proc. R. Soc. London, Ser. A*, submitted.
(8) Kennedy, J. W.; Gordon, M.; Alvarez, G. A. *Polimery (Warsaw)* **1975**, *20*, 463.
(9) Hildebrand, F. B. "Introduction to Numerical Analysis"; McGraw-Hill: New York, 1956.
(10) Huggins, M. L. *Ann. N.Y. Acad. Sci.* **1942**, *43*, 1.
(11) Flory, P. J. *J. Chem. Phys.* **1942**, *10*, 51.
(12) Kennedy, J. W.; Gordon, M.; Koningsveld, R. *J. Polym. Sci., Part C* **1972**, *39*, 43.
(13) Kennedy, J. W. *J. Polym. Sci., Part C* **1972**, *39*, 71.
(14) Koningsveld, R. Ph.D. Thesis, Leiden, 1967.
(15) Breitenbach, Von J. W.; Wolf, B. A. *Makromol. Chem.* **1967**, *108*, 263.
(16) Šolc, K. *Macromolecules* **1975**, *8*, 819.
(17) Koningsveld, R.; Stockmayer, W. H.; Kennedy, J. W.; Kleintjens, L. A. *Macromolecules* **1974**, *7*, 73.
(18) Yamakawa, H. "Modern Theory of Polymer Solutions"; Harper and Row: New York, 1971.
(19) Irvine, P. A. Ph.D. Thesis, University of Essex, 1979.
(20) Šolc, K. *Macromolecules* **1970**, *3*, 665.
(21) Koningsveld, R., private communication of results found in ref 1.
(22) Šolc, K. *Collect. Czech. Chem. Commun.* **1969**, *34*, 992.
(23) Kleintjens, L. A.; Koningsveld, R.; Stockmayer, W. H. *Br. Polym. J.* **1976**, *8*, 144.
(24) Shohat, J. A.; Tamarkind, J. D. "The Problem of Moments"; American Mathematical Society: Providence, R.I., 1950.
(25) Collins, R.; Wragg, A. *J. Chem. Phys. A, Math. Gen.* **1977**, *10*, 1441.
(26) Flory, P. J. "Statistical Mechanics of Chain Molecules"; Wiley: New York, 1969.
(27) Shen, M. *Int. Rubber Conf., Kiev* **1978**.
(28) Ferry, J. D.; Williams, M. L.; Stern, D. M. *J. Chem. Phys.* **1954**, *58*, 987.
(29) NAG, Nottingham Algorithms Group Subroutines.
(30) Gantmacher, F. R. "Matrix Theory"; Chelsea: New York, 1959; Vol. II.

Interfacial Properties of Immiscible Homopolymer Blends in the Presence of Block Copolymers

Jaan Noolandi* and Kin Ming Hong*

Xerox Research Centre of Canada, 2480 Dunwin Drive, Mississauga, Ontario, Canada L5L 1J9. *Received June 1, 1981*

ABSTRACT: The emulsifying effect of block copolymers in immiscible homopolymer blends is studied theoretically, using a general formalism for inhomogeneous multicomponent polymer systems developed earlier by the authors. The reduction in interfacial tension with increasing block copolymer concentration is calculated for a range of copolymer and homopolymer molecular weights, and comparison is made with the experimental results of Riess and co-workers on the polystyrene–polybutadiene–copolymer–styrene system. The calculated interfacial density profiles clearly show greater exclusion of the homopolymers from the interphase region as the molecular weight of the block copolymer is increased. We also estimate the critical concentration of block copolymer required for micellar aggregation in the bulk of the homopolymer.

1. Introduction

An interesting property of diblock copolymers in incompatible homopolymer blends is their behavior as emulsifying agents, similar to soap molecules at an oil–water interface. The practical importance of this observation is that outstanding mechanical properties may be obtained by properly choosing the type and molecular weight of the block copolymer to maximally lower the interfacial tension of highly incompatible homopolymers, thereby facilitating phase separation into uniformly dispersed microdomains. Early work in this area has been carried out by Riess and co-workers[1-4] and Kawai et al.[5,6] for ternary blends of polystyrene–polyisoprene with the associated block copolymer. Recently, Cohen and Ramos[7,8] have studied the influence of diblock copolymers on the structure and properties of polybutadiene–polyisoprene

0024-9297/82/2215-0482$01.25/0